PHYSICAL REVIEW B VOLUME 27, NUMBER 6 15 MARCH 1983

Self-consistent semirelativistic pseudopotential calculation of the energy bands, cohesive energy, and bulk modulus of W

D. M. Bylander and Leonard Kleinman
Department of Physics, University of Texas, Austin, Texas 78712
(Received 25 October 1982)

The energy bands, equilibrium lattice constant, cohesive energy, and bulk modulus of tungsten have been calculated using our new semirelativistic pseudopotential. The agreement with experiment is exceptionally good. This can be attributed to the pseudopotential containing all relativistic effects, except spin-orbit, to order α^2, where α is the fine-structure constant, and to our taking the exchange-correlation potential to be $V_{xc}^{val}=V_{xc}(\rho_{total})-V_{xc}(\rho_{core})$ rather than $V_{xc}^{val}=V_{xc}(\rho_{val})$.

I. INTRODUCTION

In the past few years there have been several advances in pseudopotential theory. Zunger and Cohen[1] (ZC) developed a hard-core norm-conserving pseudopotential and a soft-core norm-conserving pseudopotential was developed by Hamann, Schlüter, and Chiang[2] (HSC). These pseudopotentials yield pseudo-wave-functions which are identical to, rather than merely proportional to (as is the case for pseudopotentials based on core orthogonalization[3]), the true wave function outside the core region. Furthermore, their energy-independent form introduces negligibly small errors which can be shown to be due to the rigorous cancellation of the linear term[2] in an expansion about the energy for which the pseudopotential was created. Kleinman[4] has shown how to obtain the HSC pseudopotential from the Dirac equation so that it contains all relativistic corrections to order α^2 where α is the fine-structure constant. If one takes the weighted average of the pseudopotentials for $j=l+\frac{1}{2}$ and $j=l-\frac{1}{2}$, a semirelativistic ionic pseudopotential

$$\bar{V}_l^{ion}=(2l+1)^{-1}[(l+1)V_{l+1/2}^{ion}+lV_{l-1/2}^{ion}] \quad (1)$$

is obtained from which computations proceed identically to those with nonrelativistic pseudopotentials. We[5] have recently shown how to cast semilocal pseudopotentials of this type (i.e., local in the radial coordinate but nonlocal in the angular coordinates) into a completely nonlocal form. This not only greatly simplifies the computation of matrix elements but also allows the small error which occurs on transporting the pseudopotential to different chemical environments to be further reduced.

In this paper we compare a calculation of the energy bands, cohesive energy, and bulk modulus of tungsten made using our new pseudopotential with similar calculations made by ZC (Refs. 6 and 7) using their nonrelativistic hard-core pseudopotential. Other than the pseudopotential, our potential differs in two respects from ZC's. We use the relativistic form[8,9] of the Kohn-Sham[10] exchange potential and, for want of something better, the nonrelativistic Wigner[11] correlation potential. Because of their nonlinear nature, the valence parts of the exchange and correlation potentials cannot rigorously be separated from the total potentials as has been pointed out by Louie, Froyen, and Cohen.[12] However, when spin polarization is not a factor, the pseudopotential (especially in its nonlocal form[5]) is self-correcting for errors made in the core region. It was for a more pedestrian reason that we chose to work with exchange and correlation energy functionals and potentials of the total charge density $\rho_T=\rho_{core}+\rho_{val}$ in the frozen-core approximation $\rho_{core}\equiv\rho_{core}^{atom}$. Because the d bands of tungsten are only partially filled, ρ_{val} is nonspherical quite close to the atoms, containing short-range $l=4$ Kubic harmonics. $\rho_{val}^{1/3}$ which appears in the exchange and correlation then contains short-range $l=8$ Kubic harmonics whose Fourier expansion shows little sign of converging even with 7000 plane waves. On the other hand, in the core region $\rho_T^{1/3}\approx\rho_{core}^{1/3}+\frac{1}{3}\rho_{val}/\rho_{core}^{2/3}$ contains only a small $l=4$ component and negligible $l=8$ component. In the next section we describe our calculation and give estimates of the errors introduced by using the pseudopotential, which was constructed to be exact for a tungsten ion in a particular configuration, in the crystalline environment and the errors introduced by the use of a small Gaussian basis set. In Sec. III we compare our results with those of ZC and with experiment.

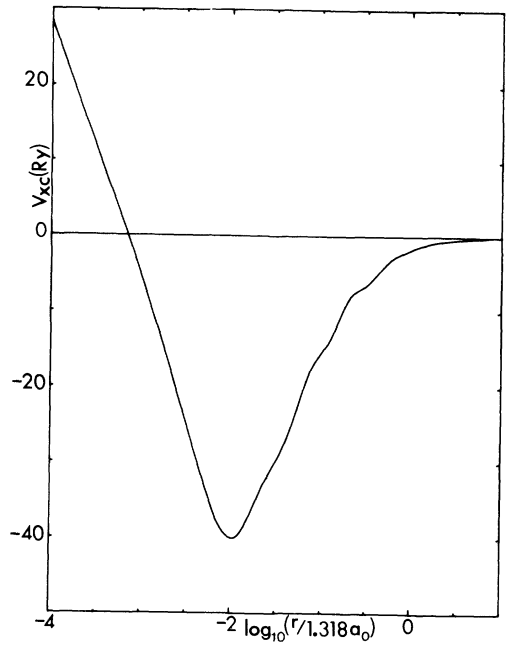

FIG. 1. Relativistic Kohn-Sham exchange plus Wigner correlation potential for $\rho_{core}(r)$ of Dirac atom.

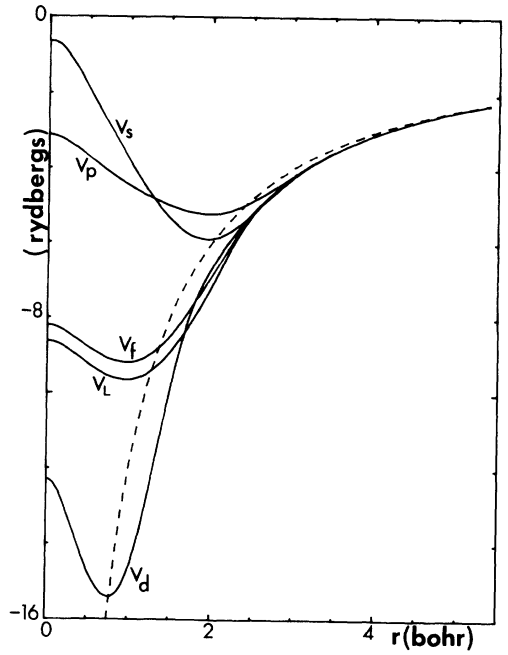

FIG. 2. Semirelativistic s, p, d, and f tungsten pseudopotentials and V_L, the local part of the pseudopotentials, together with $-2Z/r$ (dashed curve).

II. CALCULATIONAL TECHNIQUE

The atomic pseudopotentials were calculated from the Dirac equation for W^+ in the $5d_{3/2}^{1.8}5d_{5/2}^{2.7}6s_{1/2}^{0.25}6p_{1/2}^{0.083}6p_{3/2}^{0.167}$ configuration according to the prescription of Ref. 4. W^+ was used rather than W because the $5f$ functions are not bound for W in the Kohn-Sham approximation. The relativistic exchange potential (in Ry) used in the calculation is[8,9]

$$V_x(\vec{r})=-2\left[\frac{3}{\pi}\rho(\vec{r})\right]^{1/3} \times\left[\frac{3}{2}\frac{\ln[\beta+(\beta^2+1)^{1/2}]}{\beta(\beta^2+1)^{1/2}}-\frac{1}{2}\right], \quad (2)$$

where $\beta=[3\pi^2\rho(\vec{r})]^{1/3}$ α and the correlation potential[11] is

$$V_c(r)=-0.88[4\pi\rho(\vec{r})/3]^{1/3} \times\frac{\frac{4}{3}+7.79[4\pi\rho(\vec{r})/3]^{1/3}}{\{1+7.79[4\pi\rho(\vec{r})/3]^{1/3}\}^2}. \quad (3)$$

The ionic pseudopotential is obtained by subtracting the valence Coulomb potential and $V_{xc}(\rho_T)$ from the atomic pseudopotential. In order to obtain smoother potentials we subtract $V_{xc}(\rho_{core})$ from $V_{xc}(\rho_T)$. Thus $V_{xc}(\rho_{core})$ is added to the pseudopotential and subtracted from the self-consistent[13] $V_{xc}(\rho_T)$. If the reader wishes to consider

$$V_{xc}^{val}(\vec{r})=V_{xc}(\rho_T(\vec{r}))-V_{xc}(\rho_{core}(r))$$

to be a physically meaningful quantity, he may, but it is our point of view that $V_{xc}(\rho_{core})$ is an arbitrary function which is being added to one part of the potential and subtracted from another. In Fig. 1 we display $V_{xc}(\rho_{core}(r))$, where $\rho_{core}(r)$ is obtained from the Dirac equation and therefore is weakly infinite as is V_{xc} at $r=0$. In Fig. 2 we show the semirelativistic ionic pseudopotentials $\bar{V}_l^{ion}(r)$ used in this calculation. They fail to be equal to $-2Z/r$ beyond $r=3$ bohrs because of the added $V_{xc}(\rho_{core})$; although ρ_{core} is negligible in this region, $\rho_{core}^{1/3}$ is not.

The nonlocal form of the pseudopotential is generated by using $\bar{V}_l^{ion}(r)$ in a self-consistent calculation of W^+ to obtain semirelativistic pseudoeigenfunctions

$$\Phi_{lm}^0(\vec{r})=\phi_{lm}^0(r)Y_{lm}(\Omega).$$

The pseudopotential then becomes[5]

$$V_{ps}(\vec{r})=V_{xc}^{val}(\vec{r})+V_{Coul}^{val}(\vec{r})+V_L(r)+V_{NL}, \quad (4)$$

where

TABLE I. Dirac-equation eigenvalues for W^+ and W in eV and error made (in meV) when semilocal (SL) and nonlocal (NL) W^+ ionic pseudopotentials are used in self-consistent calculations for W.

	Dirac W^+	Dirac W	Δ(SL)	Δ(NL)
$5d_{3/2}$	−11.926	−4.679	13	−5.8
$5d_{5/2}$	−11.182	−4.007	12	−5.7
$6s_{1/2}$	−12.329	−6.009	−1.4	−6.1
$6p_{1/2}$	−7.639	−2.184	−6.7	−7.5
$6p_{3/2}$	−6.863	−1.733	−9.3	−10.2
$5f_{5/2}$	−1.090			
$5f_{7/2}$	−1.089			

$$V_{\mathrm{NL}}=\sum_{lm}\frac{|\delta V_l\Phi^0_{lm}\rangle\langle\Phi^0_{lm}\delta V_l|}{\langle\Phi^0_{lm}|\delta V_l|\Phi^0_{lm}\rangle}\ , \tag{5}$$

$$\delta V_l=\bar{V}_l^{\mathrm{ion}}(r)-V_L(r)\ , \tag{6}$$

and $V_L(r)$ is an arbitrary local pseudopotential chosen so that V_{ps} has good transferability. $V_L(r)$ which is shown in Fig. 2 is a numerical function, chosen to be 1.05 $\bar{V}^{\mathrm{ion}}_{l=3}(r)$ in the core and to join smoothly to $\bar{V}^{\mathrm{ion}}_{l=3}(r)$ outside the core. That it differs markedly from the V_L used in Ref. 5 is a consequence of the different $V_{\mathrm{xc}}^{\mathrm{val}}(\vec{r})$ used in the two cases. To check the transferability of the pseudopotential we calculated the eigenvalues for a W atom in the $5d^2_{3/2}5d^3_{5/2}6s^{0.5}_{1/2}6p^{0.167}_{1/2}6p^{0.333}_{3/2}$ configuration using the Dirac equation and both the semilocal and nonlocal ionic pseudopotential (arising from W^+) in a self-consistent Schrödinger-equation calculation with the results shown in Table I. (The semirelativistic pseudopotential could not be checked directly since there is no semirelativistic Dirac equation with which to compare.) The largest error arising from the nonlocal pseudopotential is −10 meV and its largest relative error is less than 5 meV. We expect the errors in the crystal to be no worse than these because the spherically averaged valance pseudo-charge-density in the core region of the crystal differs from the ion by no more than the atomic valence pseudo-charge-density does.

Our basis set consists of three s, p, and d and one f Gaussian Bloch functions for a total of only 34 basis functions. Note that Eq. (5) involves n two-center integrals whereas the semilocal form of the pseudopotential

$$\sum_{l,m}|Y_{lm}(\Omega)\rangle V_l(r)\langle Y_{lm}(\Omega)|$$

requires the computation of $n(n-1)/2$ complicated three-center integrals. Each is a single Gaussian except that the short-range d Gaussian has about 2% of a very-short-range Gaussian contracted with it. The Gaussian exponents and the contraction factor were determined by trial and error to maximize the convergence at the Γ and H high-symmetry points in the Brillouin zone (BZ). In Table II we show the convergence errors for several states at Γ and H obtained by comparing with converged-plane-wave expansions. For $\Gamma_{25'}$, our worst case, the convergence using our 34 Gaussian basis set was equivalent to that obtained using a 297 plane-wave basis set; convergence to approximately 0.2 meV required 887 plane waves. This 26-meV error is probably the largest computational error in the calculation.

TABLE II. Convergence errors at Γ and H in meV.

Γ_1	Γ_{12}	$\Gamma_{25'}$	H_{12}	$H_{25'}$	H_{15}
6.1	22.9	26.0	9.4	20.9	3.6

ZC performed sums over the BZ to obtain the Fermi energy, charge density, sum of one-electron eigenvalues, etc., using a tetrahedron integration scheme.[14] They used a 14-point sample in the $\frac{1}{48}$th irreducible BZ except for one calculation in which they used 20. They obtained a binding energy[15,16] of 16.290 07 Ry using 14 $\vec{k}$ points for W at the experimental lattice constant and at the theoretical lattice constant (estimated from 14-$\vec{k}$-point calculations) they obtained 16.265 907 Ry in a 20-$\vec{k}$-point calculation. Thus, since the equilibrium binding energy should have been the larger of the two, the energy change due to the increased number of $\vec{k}$ points was at least 0.33 eV. ZC's claims of better convergence are somewhat surprising.[17] The tetrahedral integration scheme has two flaws. (1) It joins the nth level at one $\vec{k}$ point to the nth level at a neighboring $\vec{k}$ point, ignoring possible band crossings and thus introducing energy gaps where none exist. (2) If a tetrahedron is completely below E_F, each of its four points contributes equally to the integral over the tetrahedron rather than proportionally to its proximity volume within the tetrahedron (the tetrahedra are necessarily irregular). If one sums the contribution of each point from the several tetrahedra to which it belongs, he finds that the points sampled in the BZ are misweighted.[18] We therefore sampled 50 points on a regular bcc lattice within the $\frac{1}{48}$th fcc irreducible wedge of the BZ and weight the contribution of each energy level by that fraction of a Gaussian of 0.05 eV full width at half maximum centered on the energy level which lies below E_F and by the number of independent members of the star of $\vec{k}$. Because we did not try a small sampling we cannot make an accurate estimate of the accuracy of the

sampling but it is obviously much more accurate than any 20-point sampling.

Fourier transforms of the pseudo-charge-density were obtained directly from the crystal eigenfunctions to yield

$$V_{\text{Coul}}^{\text{val}}(\vec{\mathbf{K}})=8\pi\rho(K)/K^2$$

and are summed at 360 random points in the $\frac{1}{48}$th irreducible unit cell to obtain $\rho_{\text{val}}(\vec{r})$ which is added to $\sum_i \rho_{\text{core}}(\vec{r}-\vec{\mathbf{R}}_i)$ and substituted in Eqs. (2) and (3) to obtain $V_{\text{xc}}(\rho_T(\vec{r}))$. Then

$$V_{\text{xc}}(\rho_T(\vec{r}))-\sum_i V_{\text{xc}}(\rho_{\text{core}}(\vec{r}-\vec{\mathbf{R}}_i))$$

was fitted with 140 symmetrized combinations of plane waves (SCPW) and 16 Gaussians times Kubic harmonics (four each of $l=0$, 4, 6, and 8). The rms error in the fit was always less than 8×10^{-5} eV and the largest error at any point was 3×10^{-4} eV. This fit is an order of magnitude better than we obtained when $V_{\text{xc}}^{\text{val}}$ was taken to be proportional to $\rho_{\text{val}}^{1/3}$ even though we used two additional shorter-range Gaussians for each l in that fit. The fitting functions were Fourier transformed with the same number (504) of SCPW used in $V_{\text{Coul}}^{\text{val}}(\vec{\mathbf{K}})$ to obtain $V_{\text{xc}}^{\text{val}}(\vec{\mathbf{K}})$. The valence contributions to matrix elements between Gaussian Bloch basis functions were then calculated in reciprocal space. The calculations were iterated until the largest difference between input and output potentials at any point in real space was less than 4×10^{-4} eV.

III. RESULTS

In Table III we list the various contributions to the binding energy of tungsten at the three lattice constants shown. The first row is the sum of the one-electron energies averaged over the BZ including all zeroth Fourier transforms of the potential. The arbitrary zeroth Fourier transform of the Coulomb potential (of $Z=6$ point ions with a compensating constant background of charge) is taken to be zero and subtracted from the $\sum_i V_L(\vec{r}-\vec{\mathbf{R}}_i)$ to cancel the $2Z/|\vec{r}-\vec{\mathbf{R}}_i|$ tail on the V_L's. Thus the zeroth Fourier transform of the $\sum_i V_L(\vec{r}-\vec{\mathbf{R}}_i)$ reduces to

$$(2/a^3)\int[V_L(r)+2Z/r]d^3r\ .$$

Our $\sum_{n,\vec{\mathbf{k}}}\epsilon_n(\vec{\mathbf{k}})$ cannot be directly compared with ZC's because they did not include the zeroth-exchange and correlation-potential Fourier transforms and because of differences in our pseudopotentials and exchange potentials. The next row subtracts off half the valence self-Coulomb contribution to $\sum_{n,\vec{\mathbf{k}}}\epsilon_n(\vec{\mathbf{k}})$. We would expect it to be almost equal in magnitude to ZC's $\frac{1}{2}\sum_n(\vec{\mathbf{G}})V_{\text{Coul}}(\vec{\mathbf{G}})$ which they added after subtracting off all valence self-interactions. The fact that it is almost 3 times smaller leads us to compare several Fourier components of the self-consistent pseudo-charge-density of the two calculations[19] in Table IV. It is hard to believe that the $\rho(\vec{\mathbf{K}})$ were calculated for the same crystal. On the other hand, their[7] Fig. 3 and our Fig. 3, which are contours of constant

TABLE III. Contributions to the binding energy of tungsten (in rydbergs) for three different lattice constants and the cohesive energy in eV.

a (bohr)	5.793	5.972	6.151
$\sum_{n,\vec{\mathbf{k}}}\epsilon_n(\vec{\mathbf{k}})$	6.003 770	5.362 252	4.785 872
$-\frac{1}{2}8\pi\Omega\sum_{\vec{\mathbf{K}}}'\rho^2(\vec{\mathbf{K}})/K^2$	−0.087 416	−0.117 940	−0.156 111
$-\int V_{\text{xc}}(\rho_T)\rho_{\text{val}}$	6.949 783	6.797 339	6.666 361
$\int[\epsilon_{\text{xc}}(\rho_T)\rho_T-\epsilon_{\text{xc}}(\rho_{\text{core}})\rho_{\text{core}}]$	−6.209 650	−6.072 030	−5.956 528
E_{Ewald}	−22.615 660	−21.937 796	−21.299 384
$-E_{\text{binding}}$	−15.959 173	−15.968 175	−15.959 790
E_{atom}	15.311 790	15.311 790	15.311 790
E_{cohesive}	8.807 6 eV	8.9301 eV	8.816 0 eV

TABLE IV. Comparison of several Fourier components of the self-consistent pseudocharge density ρ (in units of e/cell) obtained[19] by Zunger and Cohen in Refs. 6 and 7 and by us.

$\vec{K}$	$\rho(\vec{K})_{ZC}$ (Ref. 6)	$\rho(\vec{K})_{ZC}$ (Ref. 7)	$\rho(\vec{K})_{BK}$
0	6.0000	6.0000	6.0000
(110)	0.6905	0.6719	0.3880
(200)	−0.0235	−0.0994	−0.1523
(211)	0.0339	−0.0172	−0.1070
(220)	−0.0755	−0.0599	−0.1226
(310)	−0.1755		−0.1800
(222)	−0.0431		−0.0497
(321)	−0.0751		−0.0552

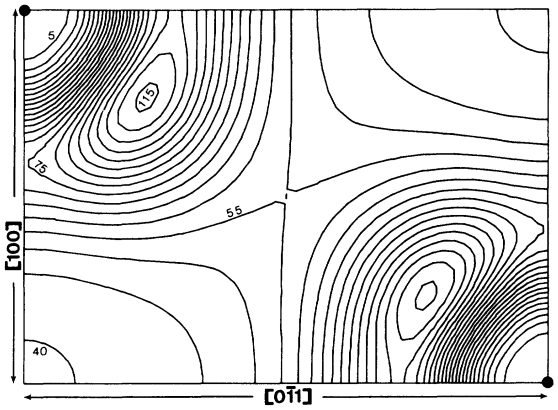

FIG. 3. Plot of contours of constant valence pseudocharge density in the (011) plane in steps of 5 millielectrons per cubic bohr.

pseudocharge-density, look quite similar.[19] Their charge density midway between second neighbors, in the center of the first neighbor bond, and at the maximum of the bond is in the ratio 1.0:1.35:3.1 and ours at the same points is 40:55:115=1.0:1.38:2.88. The next row in Table III subtracts off the one-electron exchange-energy[20] contribution to $\sum_{n,\vec{k}}\epsilon_n(\vec{k})$. Note that the

$$\sum_i V_{xc}(\rho_{core}(\vec{r}-\vec{R}_i))$$

which was subtracted from $V_{xc}(\rho_T(\vec{r}))$ does not enter here because it was added to the pseudopotential and therefore is not included in $\sum_{n,\vec{k}}\epsilon_n(\vec{k})$. The next row adds the total exchange energy minus the core exchange energy. This term was fit directly and then analytically integrated. Although, strictly speaking, in the local density approximation the core and valence exchange energy cannot be separated, subtracting that which is calculated with the core charge alone from the total yields a reasonable valence energy. In any event, the same core constant is subtracted from the atom and therefore does not affect the cohesive energy. The next row, $E_{Ewald}=-1.791\,86Z^2/R_0$ where $\frac{4}{3}\pi R_0^3=a^3/2$, represents the Coulomb energy of point ions in a constant compensating electronic background. It is because the Coulomb energy of the zeroth Fourier transform of the electronic charge is included in this term that we chose the arbitrary zeroth Fourier transform of the Coulomb potential to be zero in calculating the $\sum_{n,\vec{k}}\epsilon_n(\vec{k})$. Adding these five terms we obtain the negative of the binding energy. Subtracting the total energy of the pseudoatom from the binding energy yields the cohesive energy. The atomic energy was calculated in the $5d_\uparrow^5 6s_\uparrow$ spin-polarized[21] configuration.[22]

Fitting our three cohesive energies with a parabola we find an equilibrium lattice constant of 5.975 bohrs, a cohesive energy of 8.9301 eV, and a bulk modulus of 2.970×10^{12} dyn/cm^2. In Table V these results are compared with those of ZC (Ref. 7) and with experiment. Our agreement with the experimental bulk modulus is good and with the experimental lattice constant and cohesive energy is spectacular and probably fortuitous. The cohesive energy agreement may be due in part to the fact that no spherical approximation need be made in evaluating the atomic energy in the ground-state configuration. ZC's agreement with all three is good. Because of

TABLE V. Comparison with experiment of lattice constant (at 0 K), binding energy, cohesive energy, and bulk modulus of tungsten calculated by ZC (Ref. 7) and by us.

	ZC	BK	Expt.
a (Å)	3.173	3.162	3.162
$E_{binding}$ (Ry)	16.266	15.968	
$E_{cohesive}$ (eV)	7.90	8.930	8.90
B (erg/cm^3)	3.45×10^{12}	2.970×10^{12}	3.232×10^{12}

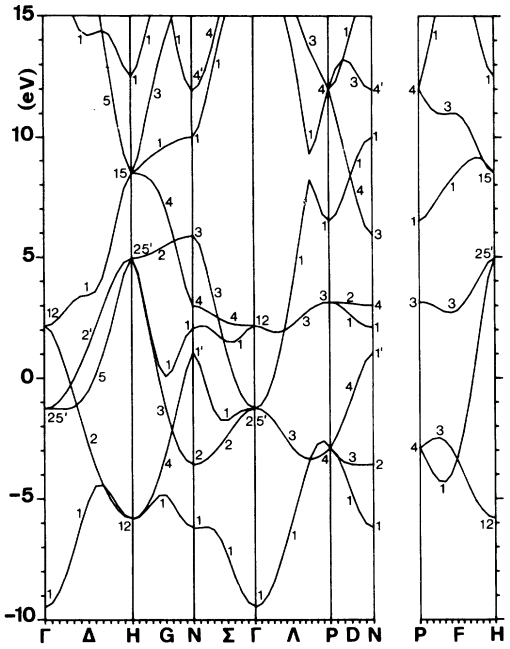

FIG. 4. Energy bands of semirelativistic tungsten with lattice constant $a=5.972$ bohrs in units of eV measured from the Fermi energy.

our more realistic treatment of the valence electron exchange energy,[12] we obtained a binding energy 4 eV smaller than ZC's and an atomic valence electron energy 5 eV smaller so that our cohesive energy is 1 eV larger than theirs. An increase of 0.0023% in the calculated binding energy at $a=5.972$ bohrs and a decrease of the same amount at $a=5.793$ bohrs

TABLE VI. Comparison of energy band eigenvalues (in eV) of tungsten as obtained by Zunger and Cohen (Ref. 6) by Petroff and Viswanathan (Ref. 23) and by us.

	ZC	PV	BK
Γ_1	0.00	0.00	0.000
$\Gamma_{25'}$	4.80	5.51	8.186
Γ_{12}	8.31	8.38	11.611
Γ_{25}	28.80	21.37	29.290
N_1	0.56	1.28	3.252
N_2	2.47	3.28	5.871
$N_{1'}$	7.89	8.64	10.497
N_1	8.21	8.67	11.519
N_4	8.92	9.28	12.435
N_3	11.03	12.16	15.339
H_{12}	0.18	0.75	3.629
$H_{25'}$	10.44	11.26	14.412
P_4	3.32	4.16	6.545
P_3	9.00	9.41	12.589
P_1	15.93	17.66	15.964

TABLE VII. Comparison of spin-orbit averaged Dirac eigenvalues (in eV) for W atom from Table I with Schrödinger-equation eigenvalues with nonrelativistic and relativistic forms of the exchange potential in the same $5d^5 6s^{1/2} 6p^{1/2}$ configuration.

	Dirac	Schrödinger rel. ex.	Schrödinger nonrel.
$5d$	−4.276	−4.816	−4.806
$6s$	−6.001	−4.752	−4.767
$6p$	−1.883	−1.739	−1.741

and $a=6.151$ bohrs are sufficient to bring the bulk modulus into agreement with experiment. Looked at in this light the agreement of the calculated bulk modulus with experiment is also quite spectacular.

Figure 4 is our calculated energy bands of semirelativistic W and in Table VI eigenvalues at symmetry points in the BZ are compared with the nonrelativistic eigenvalues of ZC (Ref. 6) and of Petroff and Viswanathan[23] (PV). The differences between the ZC and PV calculations can be attributed to the latter being made from a non-self-consistent muffin-tin potential. The differences between ZC and us should be almost entirely due to the semirelativistic nature of our pseudopotential. This gives a large s-d shift but only small relative shifts among the lower-lying pure d states. Thus our $\Gamma_{25'}$, Γ_{12}, N_2, N_4, H_{12}, and P_3 levels all lie 3.44 ± 0.15 eV higher relative to Γ_1 than do ZC's. To check how much of this s-d shift has an atomic origin in Table VII we compare the spin-orbit averaged Dirac eigenvalues for W in the $5d^5 6s^{1/2} 6p^{1/2}$ spin unpolarized configuration from Table I with all-electron Schrödinger-equation eigenvalues in the same configuration with both relativistic and nonrelativistic forms of the exchange. We see that the valence eigenvalues are not very sensitive to relativistic effects in the exchange but that the d eigenvalue is raised by 1.76 eV relative to the s on going from the completely nonrelativistic Schrödinger equation to the Dirac. Because Γ_1 is unaffected by the spin-orbit interaction and H_{12} only negligibly affected we can compare our $H_{12}-\Gamma_1$ energy difference with that of the completely relativistic but non-self-consistent calculation of Christensen and Feuerbacher.[24] They obtained 3.686 eV compared to our 3.629 eV. Thus it appears that the relativistic s-d shift in the crystal is almost twice that in the atom.

Figure 5 displays a Löwdin[25] projection of the s, p, d, and f densities of states (DOS) together with the total DOS. In order to obtain smooth curves we used the tetrahedron integration scheme here with 33 additional points along the symmetry lines

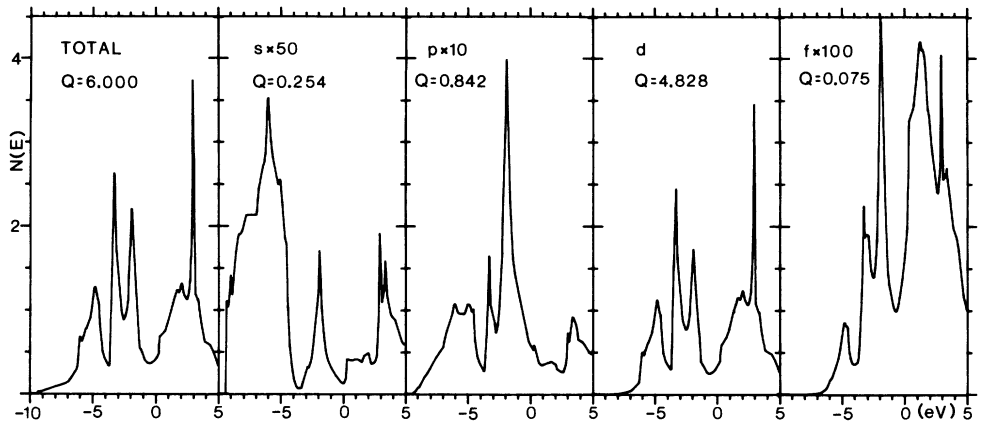

FIG. 5. Total and projected densities of states of semirelativistic tungsten. Q is the integrated charge density up to E_F.

(which were calculated for Fig. 4) added to our regular 50-point sample. The extra points along symmetry lines alleviate the band-crossing errors inherent in the tetrahedron scheme. We have previously shown[26] that the Löwdin projection, which is made onto symmetrically orthogonalized Bloch basis functions is more meaningful than other schemes. The peaks in our total DOS are in general agreement with those of ZC (Ref. 6) but differ in detail and the relativistic *s-d* shift is noticeable in a comparison of the two plots. Q, the integrated DOS (up to E_F), is shown for each projection in Fig. 5. The ratio of Q_p to Q_s is even larger for W than we[27] found for Cu. This large ratio is probably characteristic of all transition and noble metals.

In summary, we have used a new form of pseudopotential to calculate some ground-state properties of W. The pseudopotential includes all relativistic effects up to $O(\alpha^2)$ except for spin-orbit effects and is completely nonlocal, facilitating its computational use. The pseudopotential has been used with a technique which includes several noteworthy features. The pseudocharge-density is obtained directly in plane-wave expansions of Gaussian Bloch functions. The exchange and correlation potentials are evaluated numerically from the total, core-plus-valence, charge density.

In the present work the method is applied in a self-consistent calculation for W. The convergence properties of the Gaussian basis were examined together with the transferability of the pseudopotential yielding maximum errors of 26 and 10 meV, respectively. The agreement of the calculated lattice constant, cohesive energy, and bulk modulus with the experimental values is excellent. A comparison of our eigenvalues with nonrelativistic eigenvalues indicates an *s-d* shift of roughly 3.5 eV in the crystal, approximately twice that of the atom.

ACKNOWLEDGMENTS

This work was supported by The Robert A. Welch Foundation and by the National Science Foundation under Grant No. DMR-80-19518.

[1]A. Zunger and M. L. Cohen, Phys. Rev. B 18, 5449 (1978).
[2]D. R. Hamann, M. Schlüter, and C. Chiang, Phys. Rev. Lett. 43, 1494 (1979).
[3]J. C. Phillips and L. Kleinman, Phys. Rev. 116, 287 (1959).
[4]L. Kleinman, Phys. Rev. B 21, 2630 (1980).
[5]L. Kleinman and D. M. Bylander, Phys. Rev. Lett. 48, 1425 (1982).
[6]A. Zunger and M. L. Cohen, Phys. Rev. B 20, 4082 (1979).
[7]A. Zunger and M. L. Cohen, Phys. Rev. B 19, 568 (1979).
[8]A. K. Rajagopal, J. Phys. C 11, L943 (1978).
[9]A. H. MacDonald and S. H. Vosko, J. Phys. C 12, 2977 (1979).
[10]W. Kohn and L. J. Sham, Phys. Rev. 140A, 1133 (1965).
[11]E. Wigner, Phys. Rev. 46, 1002 (1934).
[12]S. G. Louie, S. Froyen, and M. L. Cohen, Phys. Rev. B 26, 1738 (1982).
[13]In the crystal it is $\sum_i V_{xc}(\rho_{core}(r-R_i))$ and not

$V_{xc}(\sum_i \rho_{core}(r-R_i))$ which must be subtracted from $V_{xc}(\rho_T(\vec{r}))$ to be consistent.

[14]G. Lehman and M. Taut, Phys. Status Solidi 54, 469 (1971).

[15]ZC call the negative of the binding energy the total energy and what is normally called the cohesive energy they call the binding energy. See Tables III and IV of Ref. 7.

[16]We thank Dr. Zunger for calling two misprints in the $a/a_0=1.00$ column of Table III, Ref. 7 to our attention. The correct values are $\sum_{j,k} N_j(\vec{k})\epsilon_j(\vec{k}) = -1.366\,59$ Ry and $E_{tot} = -16.290\,07$ Ry.

[17]Their reported differences between 14- and 20-point samplings of a 14-point calculation are an order of magnitude smaller than the difference between a 14-point sampling of a 14-point calculation and a 20-point sampling of a 20-point calculation. The 20-point sampling of the 14-point calculation is not self-consistent. Normally discrepancies between two self-consistent calculations are less than those between two calculations, one or both of which is not self-consistent.

[18]Each point should be weighted by the proximity volume within the full BZ associated with it and with the member of its star. For a regular lattice of points, this weighting is proportional to the number of independent members of the star, i.e., members which do not differ by a reciprocal lattice vector. In Table V of Ref. 6, ZC list the actual weightings obtained from the tetrahedron integration scheme for a 14-point simple cubic lattice. They find $\Lambda=(\frac{1}{4},\frac{1}{4},\frac{1}{4})$ has 6 times the weight of Γ (it should be 8) and $N=(\frac{1}{2},\frac{1}{2},0)$ has 3 times the weight of Γ (it should be 6).

[19]According to A. Zunger (private communication) the differences between the $[\rho(\vec{K})]_{ZC}$ of Refs. 6 and 7 are due in part to more optimized Gaussian exponents and better convergence in Ref. 7. Dr. Zunger also informs us that the contour labeled 0.59 in Fig. 12 of Ref. 6 should have been labeled 0.99.

[20]This term was calculated by fitting $V_{xc}(\rho_T(\vec{r}))\rho_{val}(\vec{r}) - \sum_i V_{xc}(\rho_T^{atom}(\vec{r}-\vec{R}_i))\rho_{val}^{atom}(\vec{r}-\vec{R}_i)$, integrating the fit, and adding the integral of $V_{xc}(\rho_T^{atom}(r))\rho_{val}^{atom}(r)$. The fit was an order of magnitude worse than the fit of $V_{xc}(\rho_T(\vec{r}))-\sum_i V_{xc}(\rho_{core}(\vec{r}-\vec{R}_i))$ due to the nonspherical nature of $\rho_{val}(\vec{r})$. However, the errors in the fit are of random sign and the integral should be accurate to much better than 1 meV.

[21]We replaced ρ by $2\rho_\sigma$ in the exchange-energy functions for electrons of spin σ and made an interpolation of the Wigner correlation-energy functional similar to that made by U. von Barth and L. Hedin, J. Phys. C 5, 1629 (1972), for a different correlation functional.

[22]The $5d_\uparrow^4 6s_\uparrow 6s_\downarrow$ configuration had 0.475-eV-less binding energy than the $5d_\uparrow^5 6s_\uparrow$.

[23]I. Petroff and C. R. Viswanathan, Phys. Rev. B 4, 799 (1971).

[24]N. E. Christensen and B. Feuerbacher, Phys. Rev. B 10, 2349 (1974).

[25]P. O. Löwdin, J. Chem. Phys. 18, 365 (1950).

[26]D. M. Bylander, L. Kleinman, and K. Mednick, Phys. Rev. B 25, 1090 (1982).

[27]A. Euceda, D. M. Bylander, and L. Kleinman (unpublished).